The Case for the Photocatalytic Spinning Disc Reactor as a Process Intensification Technology: Comparison to an Annular Reactor for the Degradation of Methylene Blue

Irina Boiarkina[a], Stuart Norris[b], and Darrell Alec Patterson[c]

[a]Department of Chemical Engineering, University of Auckland, Engineering Building, 20 Symonds Street, Auckland, New Zealand, *iboi002@aucklanduni.ac.nz*
[b]Department of Mechanical Engineering, University of Auckland, Engineering Building, 20 Symonds Street, Auckland, New Zealand, *s.norris@auckland.ac.nz*
[c]Corresponding Author: Nanostructured and Tuneable Materials Laboratory, Department of Chemical Engineering and Centre for Sustainable Chemical Technologies, University of Bath, Claverton Down, Bath, BA2 7AY, United Kingdom, *D.Patterson@bath.ac.uk*

Abstract

A spinning disc reactor was investigated as a process intensification technology for photocatalysis and compared with a conventional annular reactor. It was found that the average photonic efficiency achieved in the SDR was three times larger than the maximum photonic efficiency achieved in the annular reactor, 0.19±0.08% versus $0.062 \pm 0.009\%$, indicating that the SDR is significantly more efficient at utilising the incoming light. Similarly, the average volumetric rate of reaction for the SDR was an order of magnitude larger than that of the annular reactor, $3.6 \pm 1.5 \times 10^{-4}$ mol.m^{-3}.s^{-1} versus $0.13 \pm 0.02 \times 10^{-4}$ mol.m^{-3}.s^{-1}, due to the significantly smaller volume in the SDR. However, the average surface rate of reaction is more useful for comparison in an immobilised catalyst system. In the SDR, the initial surface rate of reaction was approximately the same (within the margin of error) as the photocatalytic reaction in the annular reactor. This suggests that both reactors exhibit the same rate limiting step. Given the significantly higher mass transfer rate in the SDR over the annular reactor, it is likely that the rate limiting step is either the adsorption of oxygen onto the catalyst or the electron transfer from the catalyst to the oxygen, often found to be the rate limiting step in photocatalytic reactions. However, the maximum surface rate of reaction achieved in the SDR (at a flow rate of 15mL.s^{-1}) was two times larger than the maximum reaction achieved in the annular reactor — this suggests that at this condition the rate limiting step is being overcome, and that when operated at this condition the photocatalytic SDR is performing as a process intensification technology.

Keywords: spinning disc reactor, photocatalysis, process intensification, annular reactor, reactor comparison.

1 Introduction

Process intensification is a research area that focuses on improving the efficiency and productivity of process systems [1, 2]. A variety of process intensification strategies and technologies have been investigated and a review can be found in [3]. A spinning disc reactor (SDR) is one process intensification technology that shows increased heat and mass transfer characteristics [4, 5, 6]. In an SDR, the liquid is fed centrally onto a horizontally rotating disc, whereby the centrifugal force causes the liquid to spread out into a thin liquid film.

Photocatalysis is a different research area that involves using light to take advantage of the semiconductor electron band structure, commonly used to either partially or fully degrade waste in wastewater [7]. However, traditional photocatalysis, which is conducted with powder catalysts in either annular or open channel reactors, suffers from slow kinetics and is difficult and expensive to scale up, primarily due to the need for expensive solids handling and separation equipment to deal with the powder catalyst [8, 9, 10]. Consequently, in photocatalysis, immobilised thin film catalysts have become increasingly popular to remove the need for the post separation step required with powders, however this leads to mass transfer limitations due to reduced surface area and concentration gradients in the liquid [9, 11, 10, 7, 12]. Hence the SDR has been studied as a process intensification technology for the photocatalytic treatment of waste in wastewater in order to overcome these issues [13]. This previous work investigated the effect of the flow regimes and operational parameters (flow rate and rotational speed) on the performance of the SDR and found a peak in the degradation rate at an intermediate flow rate of 15mL.s^{-1} [13]. This optimal would differ for different compounds since it depends on the photocatalytic degradability of the compound. For example, a different optimum was found for dehydroabietic acid [14].

However, so far the photocatalytic SDR has not been directly shown to be superior to other photocatalytic reactors and a process intensification technology may only be classed as such if it shows an enhancement over another process used for the same application. One of the most commonly used photocatalytic reactors for wastewater treatment applications is the annular reactor [15]. The annular reactor has been used for benchmarking the performance of novel photocatalytic systems, for example Sengupta et al. [16] used it for comparison with a Taylor vortex reactor, and Ray [17] used it for comparison with a novel reactor utilising U-shaped lamps. Therefore the aim of this work was to compare the photocatalytic performance of the SDR to the conventional annular reactor for the degradation of a well characterised model waste compound, methylene blue (a textile dye), in order to establish under what operating conditions (if any) the photocatalytic SDR is a process intensification technology. The authors acknowledge that the reactors are not the same and so there can never be an exact comparison between completely different reactors such as these. However, a comparison can made by removing the reactor dimensions and extent as much as possible by looking at parameters such as reaction rate on the basis of catalyst surface area (rather than exclusively on the basis of reaction volume or reactor volume) and photonic efficiency. Therefore factors

that look at how the photocatalyst performs in the reactor configuration are compared, rather than how the reactor performs overall, as overall performance is influenced by volume, residence time and amount and surface area of catalyst present, which differ significantly between the two reactors. Overall degradation is not used as a comparison for this reason — it too is influenced by the reactor volume and amount of catalyst in the particular reactors. By doing this, the authors put the reactors on an equal footing and consequently can compare them on as equal a basis as possible.

2 Method and Materials

2.1 Materials

Methylene blue was obtained from Sigma-Aldrich (85% pure) and 99.5% pure oxygen by BOC gases was used for saturation of the reactant solution. The reagents used for TiO_2 sol preparation were glacial acetic acid (Univar, 99.7%), acetylacetone (Sigma-Aldrich, 99%), isopropanol (Univar, 99.7%), titanium isopropoxide (Aldrich, 97%) and deionised water (from an ELGA Maxima Ultra purifier system). The solvents used for analysis with high pressure liquid chromatography were trifluoroacetic acid (Sigma-Aldrich, 99%) and acetonitrile (Merck, 99.8%). All reagents were used as received.

2.2 Analytical Methods

The concentration of methylene blue was quantified using a Shimadzu LC-20AT high pressure liquid chromatography unit (HPLC) with an Agilent Eclipse XDB-C18 column. The gradient method employed two solvents A and B. Solvent A comprised of deionised water with 0.1(v/v)% trifluoroacetic acid and Solvent B comprised of 0.01(v/v)% trifluoroacetic acid, 80(v/v)% acetonitrile and 20(v/v)% deionised water. A SPL-20A UV-vis detector was used with a detection wavelength of 662nm. The gradient method used is shown in Table 1. A flow rate of $1mL.min^{-1}$ was used with an injection volume of $50\mu L$ and an oven temperature of 25°C. The method was based on the work of Ali et al. [9].

The light transmission through the quartz sleeves was measured using a Perkin-Elmer Lambda-35 UV-Vis Spectrophotometer and quartz cuvettes. The samples were cleaned with isopropanol prior to measurement. All samples were aligned such that the light passing through the quartz sleeve would be at a normal angle (perpendicular) to the curvature of the sleeve sample.

2.3 Sol-gel Catalyst Immobilisation

The sol-gel coating process was used to immobilise the titanium dioxide on the surface of the glass discs and quartz sleeves to be used in the SDR and annular reactors respectively. The sol was made according to the method described by Ling et al. [18]. The catalyst substrate was extracted from the sol at $1mm.s^{-1}$ and then allowed to air dry for 5 minutes in the fume-hood. Both the quartz sleeves and the glass discs were then

transferred to a Clayson OM550 oven at 100 °C for 30 minutes. This process was repeated once more before the discs were transferred to a F.E. Kiln furnace with an RTC 1000 Bartlett Instruments Co. controller and the quartz sleeves to a Carbolite CTF furnace with a Eurotherm controller for calcination at 500 °C for one hour to obtain the photocatalytically active anatase crystal structure. The furnace was ramped up at a rate of 2 °C.min^{-1} to minimise cracking. Once the catalyst substrate had cooled the process was repeated once more to obtain a total of four TiO_2 layers, of which two were calcined.

2.4 Spinning Disc Reactor

2.4.1 SDR Equipment Layout

The SDR used has been described in detail elsewhere [13]. A process flow diagram and photograph of the SDR rig used can be found in Figures 1a and 1b respectively. The experiments were run with complete recycle. The liquid was pumped from a stirred reservoir, a 500mL pyrex beaker, to the reactor using a Cole-Parmer 7553-75 peristaltic pump. The liquid passed through a tightly sealed glass flask and a Liebig cooler before entering the reactor. The glass flask acted as buffer tank, dampening the pulsations. The Liebig cooler was used to maintain the reactant mixture at 26 to 27°C. All transparent components of the system were wrapped with aluminium foil to prevent photolysis of the model compounds. The liquid went through the centre of the supporting disc rotating shaft before being redirected by and flowing out of the nozzle through an annular gap with an outlet radius of 21mm, shown schemtically in Figure 1c. This ensured that the UV light was not obstructed by an inlet pipe coming in from the top. The disc diameter was 200mm and the entire SDR was enclosed in an UV tight enclosure. A 20W low pressure mercury lamp (monochromatic, peak wavelength at λ=254nmUV, Steriflow, supplied by Davey Water Products NZ, part nr. GPH369N/S) was fitted in a quartz sleeve in the reactor lid with the lamp being situated at the focus of a parabolic mirror, to improve the homogeneity of the irradiation. The liquid returned back to the reactant reservoir via gravity. The reservoir was continuously sparged with oxygen to ensure that the solution was saturated. The total volume of liquid used was 550mL, of which 150mL was initially poured into the buffer tank. The setup was run for 20 minutes in the dark to allow for the adsorption of methylene blue to reach equilibrium, before the lamp was switched on and the reaction started. The adsorption time was chosen based on control experiments, the results of which can be found in [13].

2.4.2 SDR Process and Kinetic Modelling

The overall degradation rate of the parent compound was used for modelling the reaction rate across both reactors. In order to be able to model the SDR, the volume of liquid across the spinning disc needed to be known. The Nusselt model, shown in Equation 1, was used to predict the liquid height across the surface of the disc which was then used to calculate the volume of the SDR. This model assumes fully developed laminar flow

across the surface of the disc with no shear at the gas-liquid interface [5].

$$h = \left(\frac{3Q\nu}{2\pi r^2\omega^2}\right)^{\frac{1}{3}} = \beta r^{-\frac{2}{3}} \tag{1}$$

where h is the liquid film thickness at radius r, Q is the volumetric flow rate onto the disc, ν is the kinematic viscosity, ω is the rotational speed and β is a parameter which combines all of the constants into a single variable for clarity.

A mass balance was performed on the system, as in previous work [13], by treating the reactor and the reactant reservoir as separate control volumes. It was assumed that the reactant reservoir behaved as a continuously stirred tank (CST), with the outlet concentration equal to the bulk reservoir volume concentration. The change in concentration inside the reservoir (C_{INSDR}) with respect to time is expressed by Equation 2.

$$\frac{dC_{INSDR}}{dt} = \frac{Q}{V_{CST}}(C_{OUTSDR} - C_{INSDR}) \tag{2}$$

where C_{INSDR} is the concentration inside the CST and entering the SDR, C_{OUTSDR} is the concentration exiting the SDR, Q is the flow rate and V_{CST} is the volume of the CST.

Assuming that the SDR behaves as a plug flow reactor, as discussed in previous work [13], a mass balance leads to Equation 3 for the change in concentration with respect to spinning disc radius:

$$\frac{dC}{dr} = \frac{2\pi\beta}{Q}\Upsilon r^{\frac{1}{3}} \tag{3}$$

where Υ is the overall volumetric rate of reaction and r is the disc radius. The dash notation used by Levenspiel [19] is employed in this work to signify the reaction rate basis, with no dashes (Υ) signifying a volumetric rate basis and two dashes ($\Upsilon^{''}$) signifying a surface area basis.

The analytical solution with first order kinetics can be found in [13]. Most of the reactions were found to fit second order volumetric reaction kinetics, $\Upsilon = -kC^2$ — unless stated otherwise the reader may assume that the fitted rates of reaction are second order. Substituting second order kinetics into Equation 3 and integrating between the inlet and outlet radius leads to the following expression:

$$C_{OUTSDR} = \frac{1}{\frac{2\pi\beta k}{Q}\left[R_{in}^{4/3} - R_{out}^{4/3}\right] + \frac{1}{C_{INSDR}}} \tag{4}$$

where R_{out} is the outer radius of the disc and R_{in} is the inlet nozzle radius. Equations 2 and 4 were solved numerically to fit k (reaction rate constant) iteratively using MATLAB.

2.5 Annular Reactor

2.5.1 Annular Reactor Equipment Layout

The annular reactor used was a modified, off the shelf Steriflow Domestic and Commercial UV system, model number SF300, with an outer radius of 44mm, an inner radius of 25mm and a length of 410mm. A photograph and a process flow diagram of the reactor system are shown in Figures 2a and 2b respectively.

The liquid was pumped with a peristaltic pump (Cole-Parmer, 7553-75) at a flow rate of 2L.min^{-1} (33mL.s^{-1}) from the stirred tank reservoir, a 500mL pyrex beaker, to the reactor. The outlet liquid passed through a cooling coil immersed in a tank fed by tap water (to maintain the reactor temperature at 26 to 27°C) before returning to the reactant reservoir. The experiments were run with complete recycle. The pipework was a mixture of norprene (Masterflex 064042) and polytetrafluoroethylene (PTFE) piping, used to minimise adsorption of the reaction species. The lamp used was a low pressure mercury UV lamp supplied standard with the reactor and which was the same as was used for the SDR. It was housed inside a quartz tube to isolate the lamp from the liquid. All transparent parts of the reactor (reservoirs etc.) were covered with aluminium foil to prevent ambient light from reaching the reactant and contributing to the degradation of the compound through photolysis. The reactant reservoir contents were agitated using an IKA-RCT Basic magnetic stirrer. A new quartz sleeve was fitted into the annular reactor for every reaction. The reactant reservoir was initially filled with 500mL of the reacting solution and once the pump was switched on additional liquid was added, bringing the total system volume to 1L. The reactor was run for 30 minutes in the dark to allow the system to reach adsorption equilibrium before the UV and oxygen were switched on.

2.5.2 Annular Reactor Process and Kinetic Modelling

Replacing the control volume of the SDR with that of the annular reactor, a mass balance can be performed on the annular reactor in the same way as for the SDR. Performing a mass balance on a control volume of the annular reactor leads to Equation 5, the standard equation for a plug flow reactor.

$$\frac{dC}{dx} = -\frac{\Upsilon}{U} \tag{5}$$

where C is the concentration, x is a unit length of the reactor, Υ is the overall volumetric rate of reaction and U is the velocity through the annular space.

For a first order reaction $\Upsilon = kC$. Substituting this into Equation 5 and integrating over the length of the reactor, between the inlet and outlet concentrations, the outlet concentration for the annular reactor is given by Equation 6:

$$C_{OUTAR} = C_{INAR} \exp\left(\frac{-kL}{U}\right) \tag{6}$$

where C_{INAR} is the inlet concentration into the annular reactor, C_{OUTAR} is the outlet concentration of the annular reactor, L is the length of the annular reactor and U is the liquid velocity through the reactor.

Substituting Equation 6 into the equation for the CST (Equation 2), the analytical solution for the change in concentration in the continuously stirred tank reservoir using an annular reactor with first order overall reaction kinetics is given by Equation 7:

$$C = C_0 \exp\left(\frac{Q}{V_{CST}}\left[\exp\left(\frac{-kL}{U}\right) - 1\right]t\right) \tag{7}$$

where the L/U term can be replaced with V_{AR}/Q using the continuity equation. V_{AR} is the volume of the annular reactor.

For second order kinetics, which were observed with the SDR, $\Upsilon = -kC^2$ can be substituted into Equation 5. Integrating this equation over the length of the reactor and the change in concentration between the inlet and the outlet leads to Equation 8 for the concentration exiting the annular reactor. This is analogous to Equation 4 for the SDR and was also solved in MATLAB in conjunction with Equation 2.

$$C_{OUTAR} = \frac{1}{\frac{kV_{AR}}{Q} + \frac{1}{C_{INAR}}} \tag{8}$$

2.6 Volume versus Surface Reaction Rate

The kinetic constants extracted using the modelling approach discussed above are volumetric kinetic constants, which depend on the volume of the reactor. The SDR volume is significantly smaller than the annular reactor, leading to an inequitable comparison if compared solely on a volumetric rate basis. Therefore the performance of the SDR is compared to the annular reactor using illuminated surface reaction rate kinetics. Note that only the illuminated surface area of the photocatalyst is considered here since this is the active area of the catalyst. Using the surface reaction rate eliminates the effect of the different reaction volume and flow rate per surface area, and is more appropriate for heterogeneous catalysis with an immobilised catalyst since the reaction only occurs at the catalyst surface. The surface rate of reaction can be calculated from the volumetric rate using Equation 9. The overall degradation of the parent compound is used for the quantification of the rate of reaction:

$$\Upsilon'' = \frac{V}{S}\Upsilon \tag{9}$$

where S is the illuminated surface area of the catalyst, V is the volume of solution in the reactor, Υ'' and Υ are the first or second order surface and volume rates of reaction respectively. Throughout this work, rates at two different times in the reaction are calculated for comparison between the two reactors: 1) the initial rate 2) the rate at the half life ($C = {}^1/_2C_0$) of the reaction — i.e. the rate at the time at which the concentration of methylene blue is half that of the initial concentration. This provides a better comparison between the reactors than the initial rates alone, since the effects of

deactivation will be accounted for, compared to solely using initial rates. Note that an initial rate study was not done in this work and instead a more comprehensive rate study using the reaction progress kinetic analysis approach taken in this work is the approach discussed in [20], where the entire concentration versus time data set can be used to extract information about the reaction. This allows one to produce reaction kinetics that are representative of the entire reaction progress (which is of primary concern) rather than just the initial rates which for a photocatalytic reaction will always be fastest and not representative of the reaction progress nor reaction kinetics as a whole.

2.7 Quantum Yield and Efficiency

The efficiency of the photoreaction can be described by the overall quantum yield, defined as the moles of substrate reacted per mole of absorbed light. In practice, it is difficult to quantify the rate of photon absorption, thus an alternative parameter, the photon efficiency, ξ, is used (see Equation 10). For monochromatic light this is the number of molecules transformed divided by the number of photons incident from the lamp [7, 21]. The number of photons emitted by the lamp can be measured. The photonic efficiency changes as the reaction proceeds, because the reaction rate changes due to a change in concentration. Therefore the reaction is more efficient at a higher concentration where the reaction rate is higher. This is an important consideration when comparing photonic efficiencies between different papers, because photonic efficiencies should only be compared at the same concentration. For example for a first order reaction an order of magnitude change in concentration would result in an order of magnitude change in the rate of reaction, and thus the photonic efficiency. Thus, this may result in an erroneous conclusion being drawn about the process with the higher substrate concentration having the higher photonic efficiency, when in fact they may be equal.

$$\xi = \frac{\text{rate of reaction}}{\text{einstein of light incident from lamp}} \tag{10}$$

The photonic efficiency can be used to compare the performance of the SDR to the annular reactor in terms of light use efficiency. Both reactors employ the same lamp, and the same catalyst immobilisation procedure, therefore differences in photonic efficiency should highlight key reactor design and performance differences between the two reactors.

2.8 UV Irradiance

The UV irradiance was measured in W.m^{-2} using a SUV 20.IA2Y2 photometer by IML, which was connected to a TENNA 72-7765 multimeter. The Planck relation, Equation 11, was used to determine the energy (E_p) of one mol of photons (einstein) and to convert the measured irradiance from irradiance (in W.m^{-2}) to the photon flux (in $\text{einsteins.m}^{-2}\text{.s}^{-1}$). The quantity of photons emitted by the lamp was required for calculating the photonic efficiency of the reactors.

$$E_p = \frac{hc}{\lambda}.N_A \text{ [J.einstein}^{-1}\text{]} \quad (11)$$

where h is Plank's constant (6.626×10^{-34}J.s), λ is the wavelength of the light (254nm), c is the speed of light and N_A is Avogadro's constant (6.023×10^{23}).

2.9 Repeatability and Error Bars

The majority of reactions were repeated at least twice and error bars presented in the data are the +/- one standard deviation for that respective data set. However, for non-repeated reactions, the error was taken as the *maximum* error of all available data. The fitted reactions can be found in the Supplementary Material of [14].

3 Results and Discussion

3.1 UV Irradiance Comparison

3.1.1 Spinning Disc Reactor UV Irradiance

The UV irradiance in the SDR was measured at the surface of the disc in a 3×3 grid arrangement, with each measurement being repeated three times per location, before and after the experiments. Previous work [13] only looked at the irradiance profile before the experiments, however the irradiance profile was then also measured after the completion of the experiments to assess any change. The before and after measurements agreed within the margin of error, therefore an average of the two profiles was used to calculate the irradiant flux on the surface of the spinning disc, shown in Figure 3. The peak lamp irradiance of 22.7 ± 2.9W.m^{-2} occurs at the centre axis aligned with the lamp. Although the radiation field is symmetric about the lamp axis due to the parabolic reflector, the irradiant flux decreases going outward from the central axis aligned with the lamp (Figure 3). The non-homogeneous nature of the radiation field is undesirable for reactor modelling, as this means that there is a local variation in the rate of reaction on the surface of the disc depending on the irradiant flux at that position. The maximum irradiant flux is just over one and a half times larger than the minimum, 13.9 to 22.9W.m^{-2}, which is more homogeneous as compared with other work, such as the irradiance across a vertically rotating disc reactor investigated by Dionysiou et al. [22], where the maximum was fifty times larger. The calculated average photon flux reaching the surface of the catalyst was 3.99×10^{-5} ± 5.1×10^{-6} einsteins.m^{-2}.s^{-1}.

3.1.2 Annular Reactor UV Irradiance

The annular UV light irradiance was measured at the distance of the catalyst from the lamp along different distances from the lamp edges. This was necessary as the lamp has a UV arc, which causes the intensity at the ends taper off, as shown by the UV intensity profile in the annular reactor in Figure 4. The average irradiance is significantly higher than for the SDR, with a maximum of just over 150 W.m^{-2}. This is

because the irradiance is measured right adjacent to the lamp surface, where it has not yet diffused over an increasing separation distance from the catalyst. The average photon flux reaching the surface of the catalyst in the annular reactor is $2.70\text{x}10^{-4} \pm 1.8\text{x}10^{-5}$ einsteins.m^{-2}.s^{-1}, which is an order of magnitude larger than the average photon flux reaching the surface of the catalyst in the SDR. This is due to the shorter separation distance between the lamp and catalyst surface.

3.2 Performance of Spinning Disc Reactor

A detailed discussion, including the XRD analysis and SEM images of the catalyst film, adsorption and photolysis control experiments, and the performance of the SDR can be found in [13]. The SDR has two tuneable parameters, the feed flow rate and spinning disc rotational speed. Previous work [13] found that the rate of reaction did not correlate with an increase in either the flow rate or the rotational speed, with the rate of reaction remaining fairly constant. However, two reaction rate maxima were found at the intermediate flow rate of 15mL.s^{-1}.

Previous work [14] has indicated that this is likely caused by periodic forcing from the peristaltic pump, which enhances the mass transfer and/or adsorption of oxygen to the surface of the catalyst, often found to be a rate limiting step in photocatalysis [23, 24, 25]. The enhanced oxygen would decrease electron-hole pair recombination by increasing charge separation, leading to an increase in the rate of reaction. The more homogeneous flow regime present at this flow rate would also decrease light scattering and hence increase penetration of the UV light to the catalyst surface. However, the periodic forcing effect only occurs when the flow is axisymmetric from the nozzle; non-axisymmetric flow can short-circuit the flow. The two fast reactions exhibited first order kinetics, meanwhile the remaining reactions were found to exhibit second order kinetics, therefore initial reaction rates are provided for comparison. A more detailed discussion of the kinetics can be found in [13] and [14]. The first and second order dependencies were obtained by fitting first and second order models and evaluating which model showed a better fit to the data, as shown in Figure 2 in [14]. The effect of the mean film thickness (volume divided by surface area) on the initial surface and volume rates of reaction are shown in Figures 5a and 5c respectively. The two reaction maxima can be seen and the difference in the rate of reaction becomes more significant as the reaction proceeds, as shown by Figure 5b, due to the first order kinetics of the fast reactions. For a second order reaction, if the concentration decreases by a factor of two, the reaction rate decreases by a factor of four. However, for a first order reaction if the concentration decreases by a factor of two, the rate of reaction also only decreases by a factor of two. The reaction data is tabulated in Table 2. The surface rate of reactions outside of the two maxima do not differ significantly, as shown by Figures 5a to 5b. Within the tabulated data, the maximum is the maximum that occurs at a flow rate of 15mL.s^{-1}. The data labelled 'regular maximum' refers to the reaction maxima that excludes the fast reactions at 15mL.s^{-1} and therefore is representative of the data. Similarly, the average value is the mean of the reactions that exclude the fast reactions at 15mL.s^{-1}, with the error given being one standard deviation. The data used for calculating the

regular maximum and the average rate of reaction are highlighted in red in the figures provided in the Supplementary Material. The error between experiments with different operational parameters is only slightly larger than the standard deviation found with experiments with the same operational parameters. For example, from Table 2, the error for the maximum initial surface rate of reaction is $\pm 2.6 \times 10^{-8}$mol.m^{-2}s^{-1}, which is only slightly lower than the error if all the reactions (excluding the maxima) are pooled together of $\pm 3.1 \times 10^{-8}$mol.m^{-2}s^{-1}. This shows that all experiments, aside from the experiments performed at 15mL.s^{-1}, show similar surface rate reaction kinetics.

The photonic efficiency was calculated using the average photon flux in Section 3.1.1. The data is presented in Table 2 and Figures 5d to 5f, at both the initial methylene blue initial concentration (8mg.L^{-1}) and the efficiency at half of the initial concentration. The photonic efficiency for the two reactions at 15mL.s^{-1} is significantly higher and, similar to the surface rate of reaction, the difference becomes even more significant at half the initial concentration. This further underlines that these reaction conditions represent intensification beyond the normal operation of the SDR, indicating they are the optimal conditions. Note that a significant portion of the light is wasted as heat in the reactor — a cooler was installed on the feed line in order to maintain a constant temperature throughout the reaction. This also applies for the annular reactor. Future design of a photocatalytic SDR (or annular reactor) can look at decreasing this wastage.

3.3 Performance of Annular Reactor

3.3.1 Annular Reactor Photolysis and Adsorption

Unlike the SDR, the annular reactor has only one tuneable parameter, the flow rate. The reactor was operated at a recirculation flow rate of 33mL.s^{-1}, which is a slightly higher recirculation rate than used in the SDR. Previous experiments conducted at the University of Auckland using the same annular reactor have shown that changing the flow rate from 16.7mL.s^{-1} to 33mL.s^{-1} produces a negligible effect on the rate of degradation [26].

Figure 6 shows the adsorption and photolysis data for the reaction in the annular reactor. Marked adsorption only occurs in the first 15 minutes, and after that the methylene blue in the reactor remains constant at a steady 80% of the initial concentration. The adsorption experiments were used to ensure that sufficient adsorption time was allocated for adsorption to take place before the reaction was started. Therefore in all experiments, thirty minutes of adsorption time in the dark was used.

The annular reactor showed a significant degradation of methylene blue due to photolysis, as shown in Figure 6b. More than half of the compound was degraded within two hours. This is unlike the photolysis behaviour of the SDR, which showed almost no photolytic degradation during two and a half hours [13]. The strong photolytic degradation of methylene blue in the annular reactor is probably due to the higher direct UV photon flux. There is no large separation between the UV and the reactant liquid as there is in the SDR. The annular reactor also has a larger reactor volume and longer residence time, thus the reactant is exposed to UV for a longer time period. The annular

reactor also uses the entire length of the UV lamp, whereas the SDR uses approximately two thirds, due to the size of the disc. Some of the light in the SDR would be lost as heat to the collection basin surrounding the SDR.

3.3.2 Annular Reactor Photocatalytic Degradation of Methylene Blue

Figure 7 shows the progress of the reaction with the presence of the catalyst coating. Although the presence of the catalyst increases the rate of reaction, at least half of the degradation is still possibly due to photolysis. This produces a problem in modelling the photocatalysis in the annular reactor, given its strong photolytic degradation rate, in order to make an accurate comparison between the *photocatalytic* degradation potential of the two reactors. Therefore a method was devised to account for this.

3.4 Separation of Photolysis and Photocatalysis in the Annular Reactor

According to an irradiance balance, the rate of the photolytic reaction should be lower with the presence of the catalyst than without. This is because some of the light that would have been used for the photolytic reaction would now be absorbed by the catalyst first; i.e. light is used first by the catalyst before any unabsorbed light can be used for photolysis. This can be quantified by measuring the transmission of light through the quartz sleeve.

The measured transmission of light at 254nm (the wavelength emitted by the lamp) was 84% ±6% for the uncoated quartz sleeve. This is comparable to the transmission spectra obtained for the quartz sleeve by Heraeus (quartz sleeves supplier), which is 85-88% [27]. The slightly lower value in this work compared to the manufacturer is likely due to surface defects (e.g. cleanliness, dust and/or microscratches) being present in the samples used for these experiments due to handling.

The measured transmission of light in the coated sample was 33% ±6%. This means that 60% ±8% (cumulative error) of the incoming light is no longer used for photolysis. A significant portion of the light that was originally transmitted through the quartz is absorbed by the catalyst. However, this does not imply that the photolytic reaction has decreased by a factor of two. The reason for this is that the photolytic reaction rate is not always linearly proportional to the light intensity, as demonstrated by Watts and Linden [28] and Esplugas et al. [29]. A 60% drop in irradiant flux does not necessarily equate to a 60% drop in the reaction rate, the actual drop in reaction depends on the initial level of irradiant flux. The higher the initial level of irradiant flux, the smaller the drop in the rate of reaction [28]. This is similar to the trend observed in photocatalysis with TiO_2. In general in photocatalytic studies, low pressure mercury UV lamps are not considered as having high intensity, however this may be different for photolysis and for different substrates.

Thus, two scenarios can be used for comparative purposes: one with photolysis and one without. The first case scenario excludes 60% of the photolysis reaction in the annular reactor from the total degradation observed during the photocatalytic experiments. Figure 8 shows the expected reaction with 60% of the photolysis reaction subtracted.

It can be seen that the reaction behaves similarly to the reaction in the SDR: it slows down significantly towards the end of the reaction. This is designated as the reaction without photolysis. The second scenario assumes that all of the observed degradation is due to photocatalysis alone (i.e. the photolysis is present but negligible), designated with photolysis. This scenario quantifies the overall best performance of the annular reactor. The two scenarios envelope the reactor performance.

The experimental data was fitted with both first and second order kinetic models, as both fit the data well and were used in the modelling of the SDR. However, the annular reactor showed an induction period at the start, between zero and fifteen minutes (0 – 900s), which is common in radical reactions [30]. As the induction period does not represent the true degradation kinetics, the first data point was excluded during the fitting of the data. Figures 9a and 9b show the first order and second order fit for the data excluding photolysis. The fit was carried out by minimising the sum of squared differences between the experimental and fitted data. It can be seen that the second order kinetics gave a better fit: the sum of squared differences for the second order fit was 0.04 as compared with 0.27 for first order kinetis. Figure 9d is included for comparison showing a second order fit including the data at zero time, the sum of squared differences is 0.336, which is a much poorer fit than when accounting for the induction period. Therefore, without 60% of the photolysis, the kinetics were second order, the same as for the majority of reactions across the SDR. Second order kinetics did not fit with the data including photolysis, thus only first order kinetics are presented in Figure 9c. Given the different orders of reaction fitted with and without photolysis, it is likely that the photolysis is disguising the true kinetics of the reaction. Disguised kinetics are common in photocatalysis [31].

The volumetric and surface area based rates of reaction for the annular reactor are presented in Table 3 for both the initial concentration (8mg.L^{-1}) and when the reaction progresses to half of the initial concentration. It can be seen that the reaction rates without photolysis are just under half of those with photolysis, showing that overall the photolysis contributes significantly to the degradation found in the annular reactor. This is different than when compared with the SDR, where negligible photolysis occurs and all of the degradation is due to photcatalysis only.

3.5 Photonic Efficiency in an Annular Reactor

The photonic efficiency in the annular reactor was calculated using the average photon flux presented in Section 3.1.2 and the rate of reaction at a concentration of 8mg.L^{-1}, the average initial concentration of the majority of the reactions. The photonic efficiency is presented in Table 3. Note that it is difficult to compare photonic efficiency between different studies, as it is dependent upon the concentration of the substrate.

Dijkstra [32] compared three annular reactor immobilised systems for the degradation of formic acid, and found their photonic efficiency comparable, at 27.5% for an annular reactor set up similar to this one. This is three orders of magnitude higher than that observed in this reactor. However, the concentration used by Dijkstra was an order of magnitude larger than that used in these experiments. Thus the initial degradation

rate would have been larger by the same magnitude (as the reactions had first order kinetics), explaining some of the difference. Dijkstra also selected formic acid as it is easily degraded with no by-products [33], therefore there would be no competition with intermediates for active sites.

No previous studies of the photocatalytic degradation of methylene blue in an annular reactor could be found in the available literature. However, other studies which looked at the photocatalytic degradation of other model compounds in an annular reactor are outlined in Table 4. Liquid phase reactions carried out in annular reactors however often use the powdered form of the catalyst, making the comparison not as clear cut. The photonic efficiencies shown in the first two rows of Table 4 are an order of magnitude higher than in this study, which is most likely caused by the large surface area available with a powdered form catalyst. The photonic efficiencies for an immobilised catalyst approximating that used in this study are of a similar magnitude in studies by Chester et al. [34] and Lin and Valsaraj [35] and shown in the last two rows of Table 4. Combined, Table 4 indicates that the photonic efficiencies obtained in this work are in line with others and are therefore most likely valid for comparison with the SDR.

3.6 Comparison Between SDR and Annular Reactor Performance

A process technology can only be quantified (and qualified) as a process intensification technology if it is compared against another more standard technology. So, this is done here for the photocatalytic SDR compared to the photocatalytic annular reactor. Several variables and characteristics can be compared between the two reactors including: design and operational simplicity, photonic efficiency, the surface and volume rates of reaction and mass transfer limitations. Therefore these will be examined and compared in turn.

3.6.1 Design and Operational Simplicity

The annular reactor is a mechanically simpler system that is easier to design and requires lower maintenance due to a lack of moving parts. The annular reactor also already has users around the world and so offers the opportunity to retrofit existing water and wastewater UV treatment systems which traditionally do not incorporate a photocatalyst, coating the catalyst directly onto the protective sleeve that separates the lamp from the wastewater. In contrast, the SDR is a significantly more complex system, which is difficult to design due to the shaft and motor assembly and the requirement of a parabolic reflector. It also contains moving parts, which would result in higher maintenance. Therefore from this perspective, the annular reactor is a better reactor. However, the sixth principle of Green Engineering states: "Embedded entropy and complexity must be viewed as an investment when making design choices on recycle, reuse, or beneficial disposition"[36]. Therefore good green (environmental and sustainable) design should embrace complexity, so long as there is a benefit (such as a triple bottom line benefit of cost, enviromental, social) for incorporating this added complexity. At a basic level, this indicates that the photocatalytic SDR is only beneficial and worthwhile using instead of a conventional reactor, like the annular reactor, if there is some signif-

icant process intensification. Therefore the remaining comparison variables are key to determining this.

3.6.2 Scalability

It is feasible to scale-up both reactor systems, but most likely as recirculating reactors (as they are operated in this work) rather than single pass reactors. Although recirculating reactors are not uncommon in chemical engineering, due to the intrinsically slow kinetics, the photocatalysts used cannot take full advantage of this bench-scale reactor, even with the improvement it has shown over the conventional annular reactor. The testing of different catalysts was not carried out (and is beyond the scope of this paper) and so is future work. Therefore, at this stage, the authors do not think it is feasible to use the bench scale reactors used in this study as single pass systems, unless a significantly intrinsically faster catalyst is used. A scaled up version of both reactors (i.e. an annular reactor with a larger residence time and a SDR with a larger residence time and or more SDRs in series — as you typically increase the number of rather than scale up these reactors) would however be different. These could be used as single pass systems, however with the possibility to recirculate in order to have better control over the effluent quality. However, it should be noted that whether the system (or any photocatalytic system) in question can be used as a single pass system depends on the level of treatment required, which is determined by the pollutant and the purpose of the reactor (e.g. final tertiary treatment before wastewater output into the environment or intermediate treatment to make recalcitrant waste more biodegradable for conventional biological processes).

3.6.3 Photonic Efficiencies

A comparison between the initial photonic efficiencies in the SDR and annular reactors is shown in Table 5. The photonic efficiency of the SDR is significantly higher than for the annular reactor. The average photonic efficiency achieved in the SDR is an order of magnitude higher than the maximum photonic efficiency in the annular reactor (which includes the photolysis rate). The maximum photonic efficiency in the SDR is nearly twenty times larger than the maximum photonic efficiency achieved in the annular reactor. The lamps used between the two reactors were the same, however the length of lamp utilised in the SDR was only two thirds of that used in the annular reactor. Due to the separation distance between the lamp and the catalyst in the SDR, the UV irradiance reaching the surface of the catalyst is also significantly smaller than in the annular reactor (see Section 3.1.2). This shows that the SDR uses the UV light significantly more efficiently than the annular reactor, even though the annular reactor also displays a significant photolytic degradation performance.

3.6.4 Reaction Rates

The comparison between the initial volumetric degradation rates in the two reactors is shown in Table 6. The SDR outperforms the annular reactor in terms of volumetric rate

of reaction, with the average volumetric rate of reaction of the SDR exceeding that of the annular reactor by an order of magnitude, well outside the error observed with the experiments. This is because the volume in the annular reactor is significantly larger than in the SDR.

However, a comparison of the initial surface rate of reaction between the two reactors (Table 7) shows a different result. If the average rate of reaction observed in the SDR is compared with the annular reactor rate excluding photolysis, then the surface rate of reaction is within the margin of error. This is also true for the rate at half the initial concentration. This means that approximately the same number of molecules are degraded per unit time per surface area of the catalyst in either reactor, implying that the intrinsic surface rates between the two reactors are similar and likely have the same rate limiting step. However, the maximum surface reaction rate in the SDR is significantly higher than the maximum rate found in the annular reactor (including photolysis), outside the margin of error of either set of experiments. The maximum rate of reaction found in the SDR is two times larger than the maximum rate found in the annular reactor. This implies that the overall rate limiting step in the SDR at its maximum performance is different to that found in the annular reactor. Therefore, given the complexity of the SDR, it would only be advantageous to use the SDR for photocatalysis if it is operated within the conditions that show the maximum performance.

3.6.5 Mass transfer limitations

It is often noted that the reactions in a photocatalytic system with an immobilised system show mass transfer limitations [7], and it was for the enhanced mass transfer characteristics of the SDR that it was investigated in the first place as a photocatalytic process intensification reactor system. Carbin and Gabe [37] looked at the mass transfer in an annular reactor using the same method as Burns and Jachuck [38] for the SDR, using the limiting current technique of the electrochemical deposition of copper from copper sulphate solution. They obtained a correlation for the Sherwood number for laminar flow in terms of other dimensionless groups, shown in Equation 12.

$$\mathrm{Sh} = 3.93\mathrm{Re}^{0.32}\mathrm{Sc}^{0.33} \tag{12}$$

The dimensionless groups were evaluated for the operational parameters of the annular reactor with a flow rate of 2 L.min^{-1} and inner and outer diameters of 25 and 44 mm respectively, a diffusivity of 4×10^{-10} m^2.s^{-1} for methylene blue [39] and viscosity and density of water. The numbers are presented in Table 8, based on the hydraulic diameter as the characteristic length (L), with the Sherwood number evaluated using Equation 12. Therefore the mass transfer rate, k_L, for an annular reactor, as calculated from the Sherwood number is 8.5×10^{-3} mm.s^{-1}. This is in the same order of magnitude as the mass transfer rate found by Ross and Wragg [40], of 4×10^{-3} mm.s^{-1}. Ross and Wragg [40] also looked at the mass transfer rate for turbulent flow in annuli, and found an increase of approximately ten times between laminar and turbulent flow. For example, at a Reynolds number of 10^4 the mass transfer rate for an annular reactor would

be around 1.4×10^{-2} mm.s^{-1}, however either a very large flow velocity or a significantly thinner annular gap would be required to achieve this.

Importantly however, these mass transfer rates are significantly smaller than those found in the SDR by Burns and Jachuck [38]. The mass transfer rates found on the SDR were on the order of 0.16 to 0.35 mm.s^{-1}, which are two orders of magnitude larger than found in the annular reactor. Therefore the SDR has this significant advantage over the annular photoreactor. Given that the average surface rate of reaction in the SDR is similar to the photocatalytic (excluding photolysis) rate of reaction in the annular reactor, it is unlikely that the reaction is mass transfer controlled in either reactor. Therefore there is a limitation of some other nature that is being overcome during the optimal operational parameters of the SDR, where a two fold enhancement factor is seen above the maximum surface rate of reaction observed in the annular reactor (including photolysis). Slow oxygen adsorption kinetics or slow electron transfer between the catalyst and adsorbed oxygen have often been found to be the rate limiting step in photocatalysis [23, 24, 25], and it is possible that the high rate of reaction found at the best performance of the SDR overcomes one of these limitations. Specifically that there is an enhancement in either the adsorption of the oxygen or an enhancement in the electron transfer between the catalyst and the adsorbed oxygen. Previous work [14] outlines the specific conditions and phenomena to achieve this in detail. Overall, this indicates that the photocatalytic SDR is a process intensification technology, however this only occurs at the optimal conditions with an intermediate flow rate of 15mL.s^{-1}, where periodic forcing from the peristaltic pump enhances the mass transfer and/or electron transfer of the oxygen and the more homogeneous flow regime maximises UV transmission through the fluid film for methylene blue. This may differ for different reactants and for differently designed SDRs. However, this work demonstrates that fully understanding and defining how these conditions can be achieved in photocatalytic SDRs is the most important operational characteristic if they are to be rationally and beneficially adopted as a photocatalytic process intensification technology.

4 Conclusions

The spinning disc reactor was investigated as a process intensification technology for photocatalysis by comparing it with the conventional annular reactor. From a qualitative comparison, the SDR is significantly more complex to design, build and maintain, when compared to an annular reactor, due to the presence of moving parts. It was found that the average photonic efficiency achieved in the SDR was an order of magnitude larger than the maximum photonic efficiency achieved in the annular reactor, $0.19 \pm 0.08\%$ versus $0.073 \pm 0.011\%$ respectively. This indicates that the SDR is significantly more efficient at utilising the incoming light. Similarly, the average volumetric rate of reaction for the SDR was an order of magnitude larger than that of the annular reactor, $3.6 \pm 1.5 \times 10^{-4}$ mol.m^{-3}s versus $0.13 \pm 0.02 \times 10^{-4}$ mol.m^{-3}s, due to the significantly smaller volume in the SDR. However, the average surface rate of reaction in the SDR was approximately the same, within the margin of error, as the photocatalytic reaction in the

annular reactor (excluding photolysis). This suggests that both reactors exhibit the same rate limiting step. Given the significantly higher mass transfer rate in the SDR over the annular reactor, it is likely that the rate limiting step is either the adsorption of oxygen or the electron transfer from the catalyst to the oxygen (often found to be the rate limiting step in photocatalytic reactions). However, the maximum rate of reaction achieved in the SDR was two times larger than the maximum reaction achieved in the annular reactor, 3.51 ± 0.26 versus 1.66 ± 0.22 $\times 10^7$ mol.m^{-2}.s^{-1} respectively. As the maximum reaction in the annular reactor included a strong degradation due to photolysis, which was not exhibited in the SDR, the photocatalytic rate found in the SDR exceeded both the photocatalytic and photolytic degradation found in the annular reactor. The maximum rate of reaction in the SDR occurred at a flow rate of 15mL.s^{-1}. This suggests that at this condition the rate limiting step is being overcome, and that when operated at this condition the SDR is performing as a process intensification technology for this application.

5 Acknowledgements

The authors acknowledge the University of Auckland Doctoral Scholarship supporting Irina and thank the University of Auckland for support of this work in FRDF grant (3609556/9271), as well as the University of Auckland PRESS accounts for funding the consumables. The authors also acknowledge Allan Clendinning, Ray Hoffmann, Peter Buchanan, Laura Liang and Frank Quin for technical help, the University of Auckland's Faculty of Engineering Workshop for fabricating the reactor and Jessie Mathew and Cecilia Lourdres for their administrative help at the Department of Chemical and Materials Engineering.

References

[1] C. Brechtelsbauer, N. Lewis, F. Oxley, P.and Ricard, and C. Ramshaw, "Evaluation of a spinning disc reactor for continuous processing," *Organic Process Research & Development*, vol. 5, no. 1, pp. 65–68, 2000.

[2] A. Aoune and C. Ramshaw, "Process intensification: Heat and mass transfer characteristics of liquid films on rotating discs," *International Journal of Heat and Mass Transfer*, vol. 42, no. 14, pp. 2543–2556, 1999.

[3] A. Górak and A. Stankiewicz, "Intensified reaction and separation systems," *Annual Review of Chemical and Biomolecular Engineering*, vol. 2, pp. 431–451, 2011.

[4] K. V. K. Boodhoo and R. J. Jachuck, "Process intensification: Spinning disc reactor for styrene polymerisation," *Applied Thermal Engineering*, vol. 20, no. 12, pp. 1127–1146, 2000.

[5] J. R. Burns, C. Ramshaw, and R. J. Jachuck, "Measurement of liquid film thickness and the determination of spin-up radius on a rotating disc using an electrical resistance technique," *Chemical Engineering Science*, vol. 58, no. 11, pp. 2245–2253, 2003.

[6] I. Tsibranska, D. Peshev, G. Peev, and A. Nikolova, "Modelling of mass transfer in film flow of shear thinning liquid on a horizontal rotating disk," *Chemical Engineering and Processing: Process Intensification*, vol. 48, no. 3, pp. 823–827, 2009.

[7] A. Mills and S. Le Hunte, "An overview of semiconductor photocatalysis," *Journal of Photochemistry and Photobiology A: Chemistry*, vol. 108, no. 1, pp. 1–35, 1997.

[8] T. van Gerven, G. Mul, J. Moulijn, and A. Stankiewicz, "A review of intensification of photocatalytic processes," *Chemical Engineering and Processing*, vol. 46, no. 9, pp. 781–789, 2007.

[9] A. Ali, E. A. C. Emanuelsson, and D. A. Patterson, "Photocatalysis with nanostructured zinc oxide thin films: The relationship between morphology and photocatalytic activity under oxygen limited and oxygen rich conditions and evidence for a Mars van Krevelen mechanism," *Applied Catalysis B: Environmental*, vol. 97, no. 1-2, 2010.

[10] C. McFarlane, E. A. C. Emanuelsson, A. Ali, W. Gao, and D. A. Patterson, "Understanding the rate, mechanism and reuseability of zinc oxide nanostructured films as photocatalysts for intudstrial wastewater treatment," *International Journal of Chemical Engineering*, vol. 2, pp. 63–79, 2010.

[11] A. M. Ali, E. A. C. Emanuelsson, and D. A. Patterson, "Conventional versus lattice photocatalysed reactions: Implications of the lattice oxygen participation in the liquid phase photocatalytic oxidation with nanostructured ZnO thin films on reaction products and mechanism at both 254nm and 340nm.," *Applied Catalysis B: Environmental*, vol. 106, no. 3-4, pp. 323–336, 2011.

[12] M. de los Milagros Ballari, R. Brandi, O. Alfano, and A. Cassano, "Mass transfer limitations in photocatalytic reactors employing titanium dioxide suspensions I. Concentration profiles in the bulk," *Chemical Engineering Journal*, vol. 136, pp. 50–65, 2008.

[13] I. Boiarkina, S. Pedron, and D. A. Patterson, "An experimental and modelling investigation of the effect of the flow regime on the photocatalytic degradation of methylene blue on a thin film coated ultraviolet irradiated spinning disc reactor," *Applied Catalysis B: Environmental*, vol. 110, pp. 14 – 24, 2011.

[14] I. Boiarkina, S. Norris, and D. A. Patterson, "Investigation into the effect of flow structure on the photocatalytic degradation of methylene blue and dehydroabietic acid in a spinning disc reactor," *Chemical Engineering Journal*, vol. 10.1016/j.cej.2013.02.025, 2013.

[15] A. K. Ray, H. I. de Lasa, and R. Beniot Serrano, "Photocatalytic reactor configurations for water purification: Experimentation and modeling," in *Advances in Chemical Engineering*, vol. Volume 36, pp. 145–184, Academic Press, 2009.

[16] T. K. Sengupta, M. F. Kabir, and A. K. Ray, "A Taylor vortex photocatalytic reactor for water purification," *Industrial & Engineering Chemistry Research*, vol. 40, no. 23, pp. 5268–5281, 2001.

[17] A. K. Ray, "A new photocatalytic reactor for destruction of toxic water pollutants by advanced oxidation process," *Catalysis Today*, vol. 44, no. 1-4, pp. 357–368, 1998.

[18] C. M. Ling, A. R. Mohamed, and S. Bhatia, "Performance of photocatalytic reactors using immobilized TiO_2 film for the degradation of phenol and methylene blue dye present in water stream," *Chemosphere*, vol. 57, no. 7, pp. 547–554, 2004. Times Cited: 12.

[19] O. Levenspiel, *Chemical Reaction Engineering*. Wiley, New York, 3rd ed., 1999.

[20] D. G. Blackmond, "Reaction progress kinetic analysis: A powerful methodology for mechanistic studies of complex catalytic reactions," *Angewandte Chemie*, vol. 44, no. 28, p. 4302, 2005.

[21] O. Carp, C. L. Huisman, and A. Reller, "Photoinduced reactivity of titanium dioxide," *Progress in Solid State Chemistry*, vol. 32, pp. 33–177, 2004.

[22] . D. Dionysiou, G. Balasubramanian, M. T. Suidan, A. P. Khodadoust, I. Baudin, and J.-M. Laîné, "Rotating disk photocatalytic reactor: development, characterization, and evaluation for the destruction of organic pollutants in water," *Water Research*, vol. 34, no. 11, pp. 2927–2940, 2000.

[23] A. Mills, J. Wang, and D. F. Ollis, "Dependence of the kinetics of liquid-phase photocatalysed reactions on oxygen concentration and light intensity.," *Journal of Catalysis*, vol. 243, pp. 1–6, 2006.

[24] D. F. Ollis, "Photocatalytic purification and remediation of contaminated air and water," *Surface Chemistry and Catalytics*, vol. 3, pp. 405–411, 2000.

[25] D. Monllor-Satoca, R. Gomez, M. Gonzalez-Hidalgo, and P. Salvador, "The "direct-indirect" model: An alternative kinetic approach in heterogeneous photocatalysis based on the degree of interaction of dissolved pollutant species with the semiconductor surface," *Catalysis Today*, vol. 129, pp. 247–255, 2007.

[26] N. Brewer, "Comparison of photocatalysts and reactors in the ultraviolet photocatalysed advanced oxidation of a model pulp and paper wastewater," tech. rep., University of Auckland, 2011.

[27] Heraeus-Noblelight, "Heraeus quartz glass sleeves, http:heraeus-noblelight.commediawebmedia_localmediapdfuvb122e0209_flyerquartzsleeves_ok.pdf," March 2012.

[28] M. J. Watts and K. G. L., "Chlorine photolysis and subsequent OH radical production during UV treatment of chlorinated water," *Water Research*, vol. 41, pp. 2871 – 2878, 2007.

[29] S. Esplugas, P. L. Yue, and M. I. Pervez, "Degradation of 4-chlorophenol by photolytic oxidation," *Water Research*, vol. 28, no. 6, pp. 1323–0328, 1994.

[30] G. Sivalingam, M. H. Priya, and G. Madras, "Kinetics of the photodegradation of substituted phenols by solution combustion synthesised TiO_2," *Applied Catalysis B: Environmental*, vol. 51, pp. 67–76, 2004.

[31] D. F. Ollis, "Kinetic disguises in heterogeneous photocatalysis," *Topics in Catalysis*, vol. 35, pp. 217–223, 2005.

[32] M. F. J. Dijkstra, H. Buwalda, A. W. F. de Jong, A. Michorius, J. G. M. Winkelman, and A. A. C. M. Beenackers, "Experimental comparison of three reactor designs for photocatalytic water purification," *Chemical Engineering Science*, vol. 56, no. 2, pp. 547–555, 2001.

[33] M. F. J. Dijkstra, H. J. Panneman, J. G. M. Winkelman, J. J. Kelly, and A. A. C. M. Beenackers, "Modeling the photocatalytic degradation of formic acid in a reactor with immobilized catalyst," *Chemical Engineering Science*, vol. 57, no. 22-23, pp. 4895–4907.

[34] G. Chester, M. Anderson, H. Read, and S. Esplugas, "A jacketed annular membrane photocatalytic reactor for wastewater treatment: degradation of formic acid and atrazine," *Journal of Photochemistry and Photobiology A: Chemistry*, vol. 71, pp. 291–297, 1993.

[35] H. F. Lin and K. T. Valsaraj, "A titania thin film annular photocatalytic reactor for the degradation of polycyclic aromatic hydrocarbons in dilute water streams," *Journal of Hazardous Materials*, vol. 99, no. 2, pp. 203–219, 2003.

[36] P. T. Anastas and J. B. Zimmerman, "Design through the twelve principles of green engineering," *Environmental Science & Technology*, vol. 37, no. 5, pp. 94A–101A, 2003.

[37] D. C. Carbin and D. R. Gabe, "Electrochemical mass transfer in an annulus," *Electrochimica Acta*, vol. 19, pp. 653–654, 1974.

[38] J. R. Burns and R. J. J. Jachuck, "Determination of liquid-solid mass transfer coefficients for a spinning disc reactor using a limiting current technique," *International Journal of Heat and Mass Transfer*, vol. 48, no. 12, pp. 2540–2547, 2005.

[39] J. D. Bronzino, *The biomedical engineering handbook*. CRC Press LLC Boca Raton and Springer-Verlag GmbH & Co. KG Heidelberg, 2000.

[40] T. K. Ross and A. A. Wragg, "Electrochemical mass transfer studies in annuli," *Electrochimica Acta*, vol. 10, pp. 1093–1106, 1965.

[41] G. Li Puma, V. Puddu, H. Tsang, A. Gora, and B. Toepfer, "Photocatalytic oxidation of multicomponent mixtures of estrogens (estrone(E1) 17β-estradiol (E2), 17α-ethynylestradiol (EE2) and estriol (E3)) under UVA and UVC radiation: Photon absorption, quantum yields and rate constants independent of photon absorption.," *Applied Catalysis B: Environmental*, vol. 99, pp. 388–397, 2010.

[42] M. Salaices, B. Serrano, and H. I. de Lasa, "Photocatalytic conversion of phenolic compounds in slurry reactors," *Chemical Engineering Science*, vol. 59, no. 1, pp. 3–15, 2004.

List of Figures

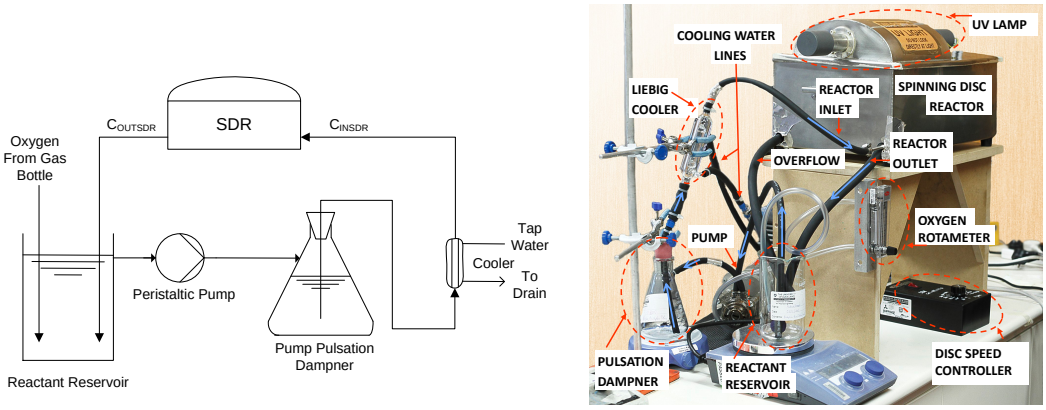

(a) (b)

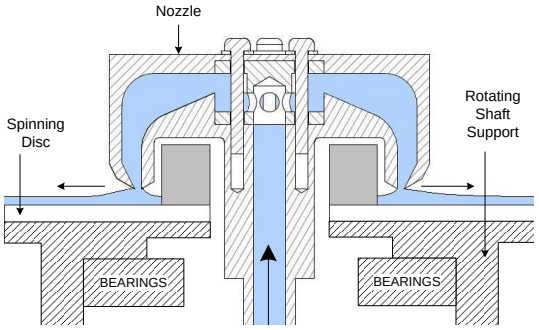

(c)

Figure 1: SDR experimental set up showing a) process flow diagram of the SDR rig b) photograph of set up c) cross-section of the inside nozzle and disc arrangement.

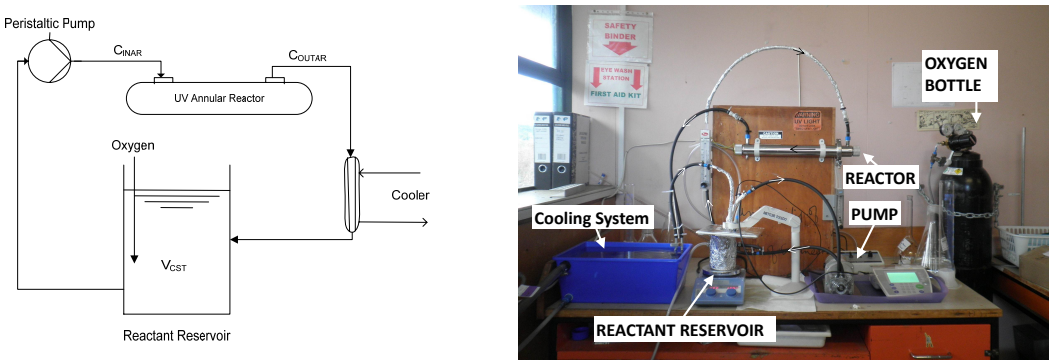

(a) (b)

Figure 2: Annular reactor experimental set up showing a) annotated photograph of reactor b) process flow diagram.

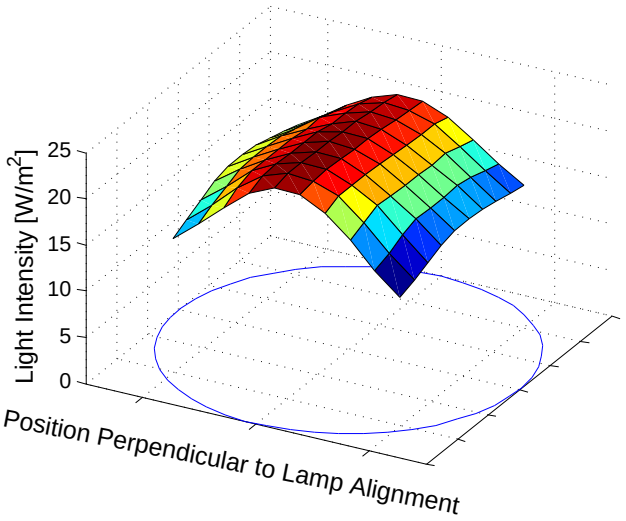

Figure 3: Measured UV light irradiance inside the spinning disc reactor.

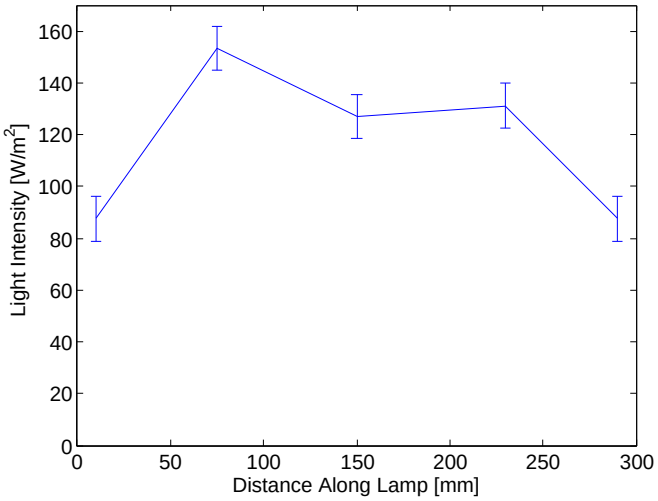

Figure 4: Measured UV light irradiance along different distances from the lamp ends.

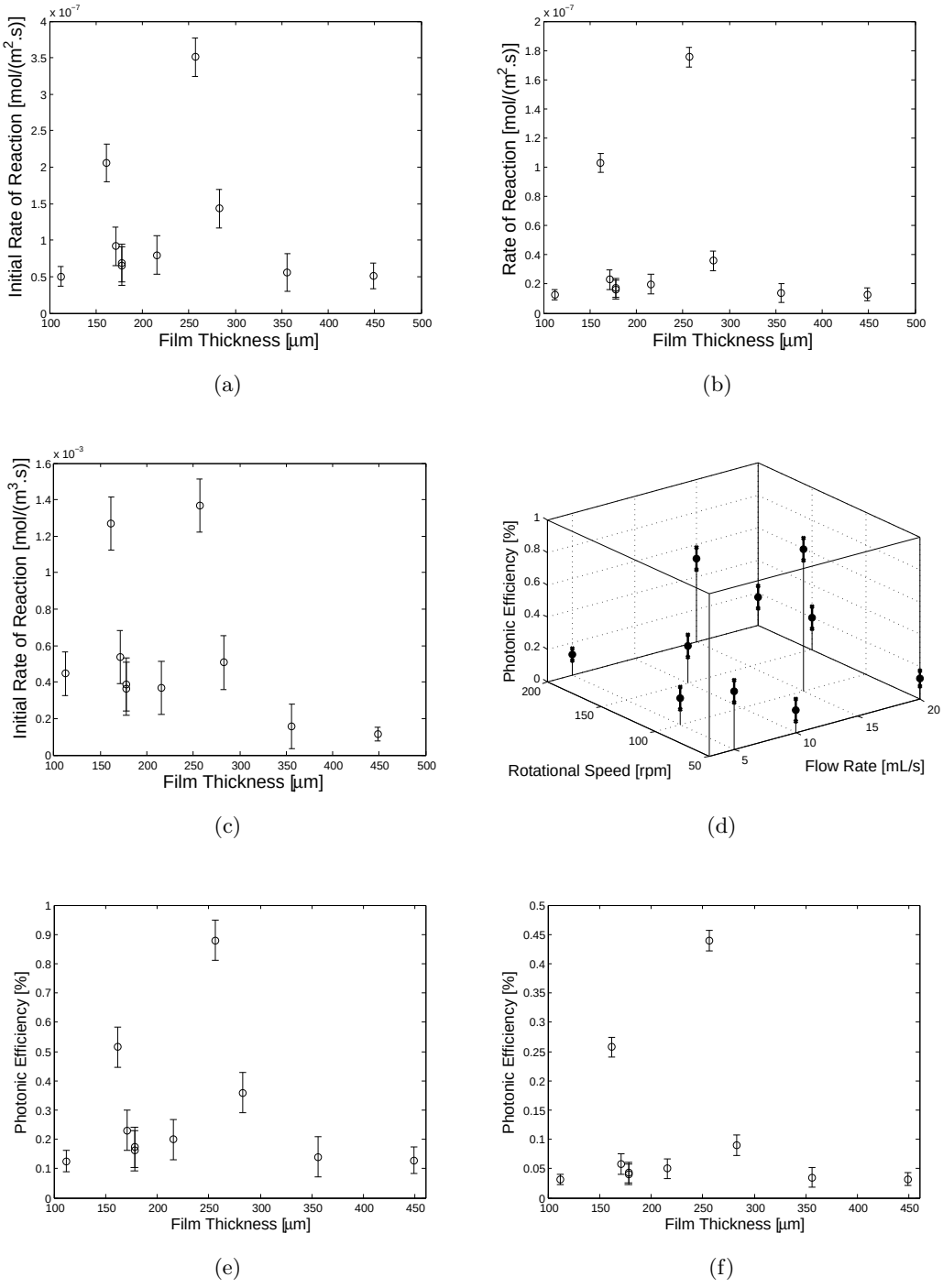

Figure 5: Experiments conducted with methylene blue in SDR showing a) effect of predicted liquid film thickness on the initial surface rate of reaction b) effect of predicted liquid film thickness on the surface rate of reaction when the reaction reaches half the initial concentration c) effect of predicted liquid film thickness on the initial volume rate of reaction d) effect of flow rate and rotational speed on the initial photonic efficiency e) effect of predicted liquid film thickness on the initial photonic efficiency f) effect of predicted liquid film thickness on the photonic efficiency when the reaction reaches half the initial concentration.

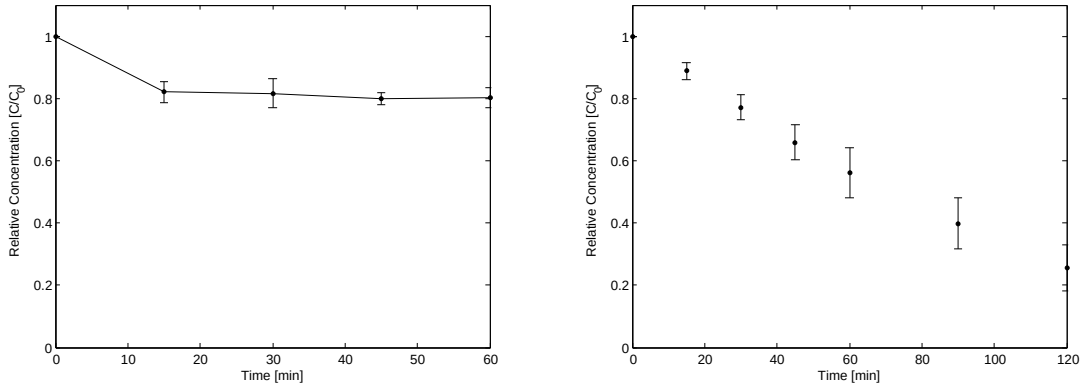

(a) (b)

Figure 6: Annular reactor control experiments at a flow rate of 33mL.s^{-1} a) adsorption study onto the reactor and catalyst b) photolysis reaction in the presence of oxygen without catalyst.

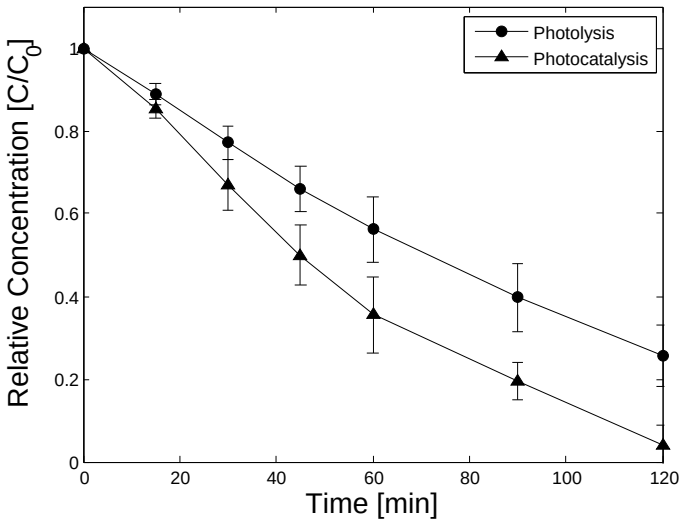

Figure 7: Degradation of methylene blue in annular reactor showing the reactions both with and without the catalyst.

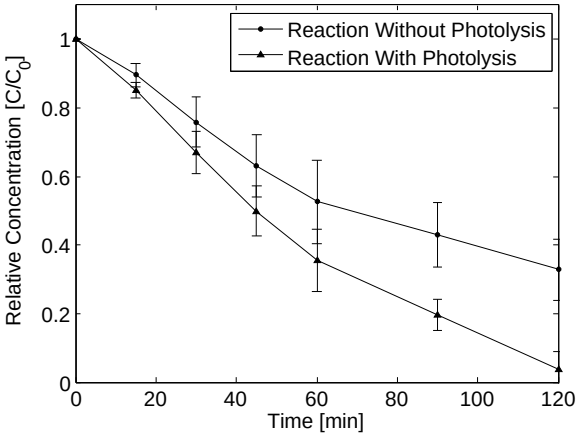

Figure 8: Comparison between the observed reaction and the observed reaction less 60% of the photolysis in annular reactor.

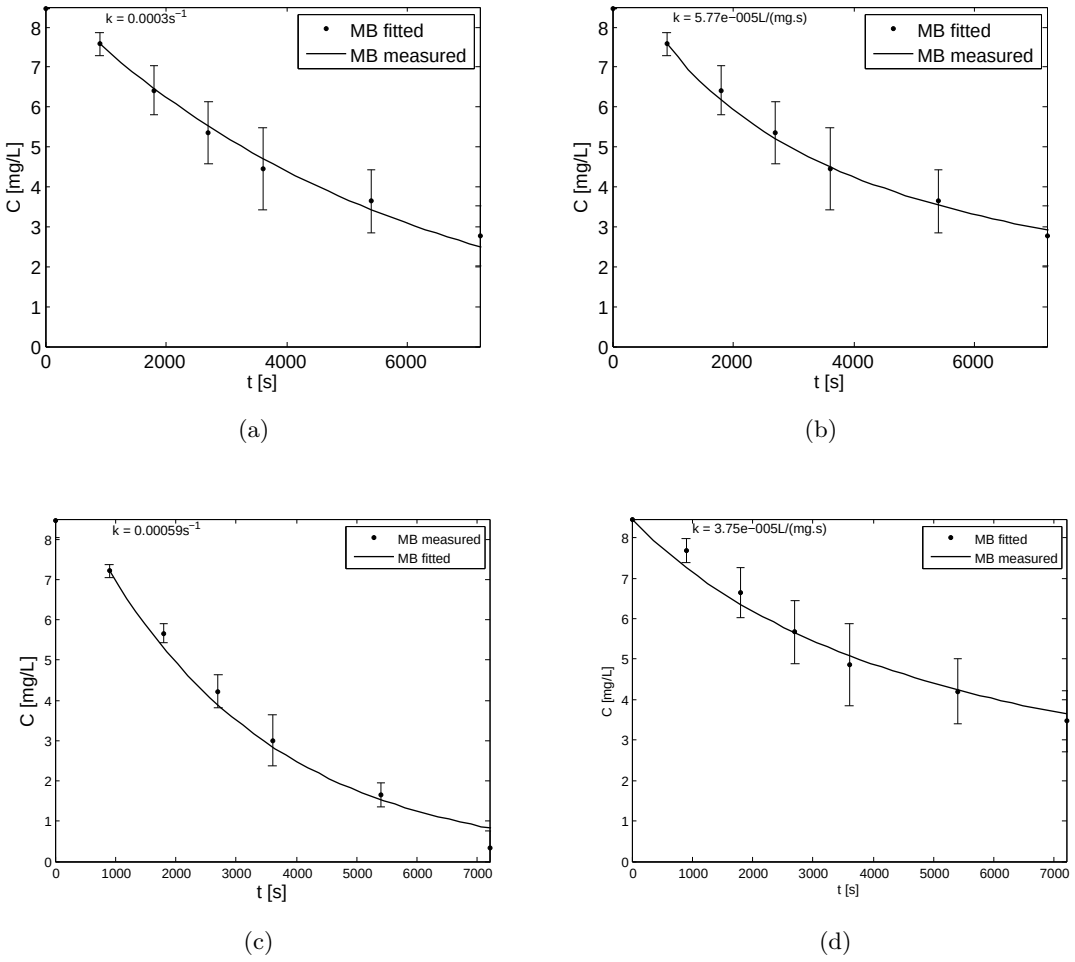

Figure 9: Experimental data fitted with the model in annular reactor a) first order, without photolysis b) second order, without photolysis c) first order, without photolysis d) second order fit, without photolysis showing induction period in first fifteen minutes.

List of Tables

Table 1: HPLC gradient method used for the quantification of methylene blue.

Time	**Concentration of Solvent A**
0 min	95%
5 min	90%
40 min	10%
45 min	95%
50 min total analysis time	

Table 2: Summary of the Performance Characteristics of the SDR.

Rate Description	**Initial Rate of Reaction $C=C_0$**	**Rate of Reaction at Half the Initial Concentration $C=1/2C_0$**
Surface Rates of Reaction $\times 10^7$ **mol.m^{-2}.s^{-1}**		
Overall Maximum	3.51 ± 0.26	1.75 ± 0.065
Regular Maximum	1.43 ± 0.26	0.358 ± 0.065
Minimum	0.501 ± 0.14	0.125 ± 0.034
Average*	0.756 ± 0.31	0.189 ± 0.077
Volume Rates of Reaction $\times 10^4$ **mol.m^{-3}.s^{-1}**		
Overall Maximum$^+$	14.0 ± 1.5	6.83 ± 0.37
Regular Maximum	5.36 ± 1.5	1.34 ± 0.37
Minimum	1.14 ± 0.38	0.285 ± 0.095
Average*	3.60 ± 1.5	0.90 ± 0.38
Photonic Efficiency %		
Overall Maximum$^+$	0.88 ± 0.07	0.44 ± 0.02
Regular Maximum	0.36 ± 0.07	0.09 ± 0.02
Minimum	0.13 ± 0.05	0.03 ± 0.01
Average*	0.19 ± 0.08	0.05 ± 0.02
*Excluding the two outlying maxima at 15mL.s^{-1}. $^+$Found to follow first order kinetics.		

Table 3: Summary of the Performance Characteristics of the Annular Reactor.

Rate Description	**Initial Rate of Reaction C=C_0**	**Rate of Reaction at Half the Initial Concentration C=$^1/_2C_0$**
Surface Rates of Reaction $\times 10^7$ **mol.m^{-2}.s^{-1}**		
Excluding Photolysis	1.29 ± 0.24	0.32 ± 0.06
Including Photolysis	1.66 ± 0.22	0.83 ± 0.11
Volume Rates of Reaction $\times 10^4$ **mol.m^{-3}.s^{-1}**		
Excluding Photolysis	0.099 ± 0.018	0.025 ± 0.018
Including Photolysis	0.13 ± 0.02	0.063 ± 0.013
Photonic Efficiency %		
Excluding Photolysis	0.057 ± 0.011	0.014 ± 0.003
Including Photolysis	0.073 ± 0.011	0.037 ± 0.006

Table 4: Photonic Efficiencies Found by Other Authors for Similar Annular Reactor Systems.

Source	**Photonic Effiency or Yield %**	**Notes**
Li Puma et al. [41]	Photonic Yield - 0.21–0.39%	Estrogen degradation, four ringed structures, similarly large to methylene blue but low solubility. Light source was at 254nm and intensity at the wall was comparable at 113.5W.m^{-2}. Degussa P25 powder used as the catalyst.
Salaices et al. [42]	Photonic Effieciency 0.94–1.67%	Phenol, 158 - 416 μmol.L^{-1}, degradation using Degusa P25 powder.
Chester et al. [34]	Photonic Efficiency 0.0049%	Degradation of atrazine in an annular reactor with an immobilized catalyst membrane on the inner wall and a medium pressure mercury lamp. They also studied the degradation of formic acid and found the photonic yield to be 0.21%, two orders of magnitude higher than for atrazine.
Lin and Valsaraj [35]	Photonic efficiency 0.0037–0.027%	Degradation of phenanthrene and pyrene in an annular reactor with external lamps and an internal coated quartz rod. Low photonic efficiency attributed to dilute concentration in the order of 0.77–6.7 μmol.L^{-1} (about 3–24 times smaller than that used in our reactor)

Table 5: Comparison of the Photonic Efficiency Between the Spinning Disc and Annular Reactors.

SDR Photonic Efficiency		**Annular Reactor Photonic Efficiency**	
Maximum	$0.88 \pm 0.07\%$	Including Photolysis	$0.073 \pm 0.011\%$
Average*	$0.19 \pm 0.08\%$	Excluding Photolysis	$0.057 \pm 0.011\%$
SDR Photonic Efficiency		* Excluding the maxima at 15 $mL.s^{-1}$	

Table 6: Comparison Between Volumetric Rates of Reaction in the Spinning Disc and Annular Reactors.

SDR Volume Rate		**Annular Reactor Volume Rate**	
Initial Rates of Reaction $[\times 10^4$ mol.m^{-3}s$^{-1}]$ (C=C$_0$)			
Maximum	14 ± 1.5	Including Photolysis	0.13 ± 0.02
Average	3.60 ± 1.5	Excluding Photolysis	0.099 ± 0.018
Rates of Reaction at Half the Initial Concentration $[\times 10^4$ mol.m^{-3}s$^{-1}]$ (C=$^1/_2$C$_0$)			
Maximum	6.83 ± 0.37	Including Photolysis	0.063 ± 0.013
Average	0.90 ± 0.38	Excluding Photolysis	0.025 ± 0.018

Table 7: Comparison Between Surface Rates of Reaction in the Spinning Disc and Annular Reactors.

SDR Surface Rate		**Annular Reactor Surface Rate**	
Initial Rates of Reaction $[\times 10^4$ mol.m^{-3}s$^{-1}]$ (C=C$_0$)			
Maximum	3.51 ± 0.26	Including Photolysis	1.66 ± 0.22
Average	0.76 ± 0.31	Excluding Photolysis	1.29 ± 0.24
Rates of Reaction at Half the Initial Concentration $[\times 10^4$ mol.m^{-3}s$^{-1}]$ (C=$^1/_2$C$_0$)			
Maximum	1.75 ± 0.07	Including Photolysis	0.83 ± 0.11
Average	0.189 ± 0.077	Excluding Photolysis	0.32 ± 0.06

Table 8: Dimensionless Numbers Used for the Calculation of the Mass Transfer Rate in the Annular Reactor

Dimensionless Group	**Definition**	**Value**
Reynolds (Re)	$\frac{\rho U L}{\mu}$	615
Schmidt (Sc)	$\frac{\mu}{\rho D}$	2500
Sherwood (Sh)	$\frac{k_L L}{D}$	406